



Soil Moisture Active Passive (SMAP)

Algorithm Theoretical Basis Document

Level 3 Radar Freeze/Thaw Data Product

(L3_FT_A)

Revision A
December 9, 2014

Scott Dunbar, Xiaolan Xu, Andreas Colliander, Kyle McDonald, Erika Podest, Eni Njoku
Jet Propulsion Laboratory
California Institute of Technology
Pasadena, CA

John Kimball and Youngwook Kim
Flathead Lake Biological Station
University of Montana
Polson, MT

Chris Derksen
Climate Research Division, Environment Canada
Toronto, Canada



Jet Propulsion Laboratory
California Institute of Technology

© 2014. All rights reserved.

The SMAP Algorithm Theoretical Basis Documents (ATBDs) provide the physical and mathematical descriptions of algorithms used in the generation of SMAP science data products. The ATBDs include descriptions of variance and uncertainty estimates and considerations of calibration and validation, exception control and diagnostics. Internal and external data flows are also described.

The SMAP ATBDs were reviewed by a NASA Headquarters review panel in January 2012 with initial public release later in 2012. The current version is Revision A. The ATBDs may undergo additional version updates after SMAP launch.

Table of Contents

ACRONYMS AND ABBREVIATIONS	4
1 INTRODUCTION	5
1.1 THE SOIL MOISTURE ACTIVE PASSIVE (SMAP) MISSION	5
1.1.1 BACKGROUND AND SCIENCE OBJECTIVES	5
1.1.2 MEASUREMENT APPROACH	5
1.2 SMAP REQUIREMENTS RELATED TO FREEZE/THAW STATE	8
2 BACKGROUND AND HISTORICAL PERSPECTIVE	9
2.1 PRODUCT/ALGORITHM OBJECTIVES.....	10
2.2 L3_FT_A PRODUCTION	13
2.3 DATA PRODUCT CHARACTERISTICS	14
3 PHYSICS OF THE PROBLEM	16
3.1 SYSTEM MODEL	16
3.2 RADIATIVE TRANSFER AND BACKSCATTER	17
4 RETRIEVAL ALGORITHM	18
4.1 THEORETICAL DESCRIPTION	18
4.1.1 BASELINE ALGORITHM: SEASONAL THRESHOLD APPROACH.....	18
4.1.2 VARIANCE AND UNCERTAINTY ESTIMATES	19
4.2 PRACTICAL CONSIDERATIONS.....	21
4.2.1 PROCESSING AND DATA FLOW CONSIDERATIONS.....	21
4.2.2 ANCILLARY DATA AVAILABILITY/CONTINUITY	21
4.2.3 UPDATING AND OPTIMIZATION OF REFERENCES AND THRESHOLDS	22
4.2.4 CALIBRATION AND VALIDATION	24
4.2.5 ALGORITHM BASELINE SELECTION.....	27
5 CONSTRAINTS, LIMITATIONS, AND ASSUMPTIONS	27
6 REFERENCES	29
APPENDIX 1: GLOSSARY	33

ACRONYMS AND ABBREVIATIONS

AMSR	Advanced Microwave Scanning Radiometer
ASF	Alaska Satellite Facility
ATBD	Algorithm Theoretical Basis Document
CONUS	Continental United States
CMIS	Conical-scanning Microwave Imager Sounder
DAAC	Distributed Active Archive Center
DCA	Dual Channel Algorithm
DEM	Digital Elevation Model
EASE	Equal Area Scalable Earth [grid]
ECMWF	European Center for Medium-Range Weather Forecasting
EOS	Earth Observing System
ESA	European Space Agency
GEOS	Goddard Earth Observing System (model)
GMAO	Goddard Modeling and Assimilation Office
GSFC	Goddard Space Flight Center
JAXA	Japan Aerospace Exploration Agency
JPL	Jet Propulsion Laboratory
LTAN	Local Time of Ascending Node
LTDN	Local Time of Descending Node
MODIS	MODerate-resolution Imaging Spectroradiometer
NCEP	National Centers for Environmental Prediction
NDVI	Normalized Difference Vegetation Index
NEE	Net ecosystem exchange
NPOESS	National Polar-Orbiting Environmental Satellite System
NPP	NPOESS Preparatory Project
NSIDC	National Snow and Ice Data Center
NWP	Numerical Weather Prediction
OSSE	Observing System Simulation Experiment
PDF	Probability Density Function
PGE	Product Generation Executable
RFI	Radio Frequency Interference
RVI	Radar Vegetation Index
SAR	Synthetic Aperture Radar
SDT	(SMAP) Science Definition Team
SDS	(SMAP) Science Data System
SMAP	Soil Moisture Active Passive
SMOS	Soil Moisture Ocean Salinity (mission)
SNR	Signal to Noise Ratio
SRTM	Shuttle Radar Topography Mission
USGS	United States Geological Survey
VWC	Vegetation Water Content

1 INTRODUCTION

The L3_FT_A product provides a daily classification of freeze/thaw state for land areas north of 45°N derived from the SMAP high-resolution radar output to 3 km polar and global EASE grids. This document provides a complete description of the algorithm used to generate the SMAP Level 3 land surface freeze/thaw product, including the physical basis, theoretical description and practical considerations for implementing the algorithm. Details of the algorithm implementation and validation approach for determining algorithm performance against the mission requirement are also included.

1.1 THE SOIL MOISTURE ACTIVE PASSIVE (SMAP) MISSION

1.1.1 BACKGROUND AND SCIENCE OBJECTIVES

The National Research Council's (NRC) Decadal Survey, *Earth Science and Applications from Space: National Imperatives for the Next Decade and Beyond*, was released in 2007 after a two year study commissioned by NASA, NOAA, and USGS to provide them with prioritization recommendations for space-based Earth observation programs [National Research Council, 2007]. Factors including scientific value, societal benefit and technical maturity of mission concepts were considered as criteria. SMAP data products have high science value and provide data towards improving many natural hazards applications. Furthermore SMAP draws on the significant design and risk-reduction heritage of the Hydrosphere State (Hydros) mission [Entekhabi et al., 2004]. For these reasons, the NRC report placed SMAP in the first tier of missions in its survey. In 2008 NASA announced the formation of the SMAP project as a joint effort of NASA's Jet Propulsion Laboratory (JPL) and Goddard Space Flight Center (GSFC), with project management responsibilities at JPL. The target launch date is January 2015 [Entekhabi et al., 2010].

The SMAP science and applications objectives are to:

- Understand processes that link the terrestrial water, energy and carbon cycles;
- Estimate global water and energy fluxes at the land surface;
- Quantify net carbon flux in boreal landscapes;
- Enhance weather and climate forecast skill;
- Develop improved flood prediction and drought monitoring capabilities.

1.1.2 MEASUREMENT APPROACH

Table 1 is a summary of the SMAP instrument functional requirements derived from its science measurement needs. The goal is to combine the attributes of the radar and radiometer observations (in terms of their spatial resolution and sensitivity to soil moisture, surface roughness, and vegetation) to estimate soil moisture at a resolution of 10 km, and freeze/thaw state at a resolution of 3 km.

Table 1. SMAP Mission Requirements

Scientific Measurement Requirements	Instrument Functional Requirements
Soil Moisture: $\sim \pm 0.04 \text{ m}^3 \text{ m}^{-3}$ volumetric accuracy (1-sigma) in the top 5 cm for vegetation water content $\leq 5 \text{ kg m}^{-2}$; Hydrometeorology at $\sim 10 \text{ km}$ resolution; Hydroclimatology at $\sim 40 \text{ km}$ resolution	L-Band Radiometer (1.41 GHz): Polarization: V, H, T_3 and T_4 Resolution: 40 km Radiometric Uncertainty*: 1.3 K L-Band Radar (1.26 and 1.29 GHz): Polarization: VV, HH, HV (or VH) Resolution: 10 km Relative accuracy*: 0.5 dB (VV and HH) Constant incidence angle** between 35° and 50°
Freeze/Thaw State: Capture freeze/thaw state transitions in integrated vegetation-soil continuum with two-day precision, at the spatial scale of landscape variability ($\sim 3 \text{ km}$)	L-Band Radar (1.26 GHz and 1.29 GHz): Polarization: Total Power (HH+VV+HV) Resolution: 3 km Relative accuracy*: 0.7 dB (1 dB per channel if 2 channels are used) Constant incidence angle** between 35° and 50°
Sample diurnal cycle at consistent time of day (6am/6pm Equator crossing); Global, ~ 3 day (or better) revisit; Boreal, ~ 2 day (or better) revisit	Swath Width: $\sim 1000 \text{ km}$ Minimize Faraday rotation (degradation factor at L-band)
Observation over minimum of three annual cycles	Baseline three-year mission life
* Includes precision and calibration stability ** Defined without regard to local topographic variation	

The SMAP spacecraft is designed for a 685-km circular, sun-synchronous orbit, with equator crossings at 6 AM and 6 PM local time. The instrument combines radar and radiometer subsystems that share a single feedhorn and parabolic mesh reflector (Fig. 1). The radar operates with VV, HH, and HV transmit-receive polarizations, and uses separate transmit frequencies for the H (1.26 GHz) and V (1.29 GHz) polarizations. The radiometer operates with polarizations V, H, and the third and fourth Stokes parameters, T_3 , and T_4 , at 1.41 GHz. The T_3 -channel measurement is used to assist in the correction of Faraday rotation effects. The reflector is offset from nadir and rotates about the nadir axis at 14.6 rpm, providing a conically scanning antenna beam at a surface incidence angle of approximately 40° . The provision of constant incidence angle across the swath simplifies the data processing and enables accurate repeat-pass estimation of soil moisture and freeze/thaw change. The reflector diameter is 6 m, providing a radiometer footprint of approximately 40 km (root-ellipsoidal area) defined by the one-way 3-dB beamwidth. The two-way 3-dB beamwidth defines the real-aperture radar footprint of approximately 30 km. The real-aperture ('lo-res') swath width of 1000 km provides global coverage within 3 days or less equatorward of 35°N/S and 2 days poleward of 55°N/S . The real-aperture radar and radiometer data will be collected globally during both ascending and descending passes.

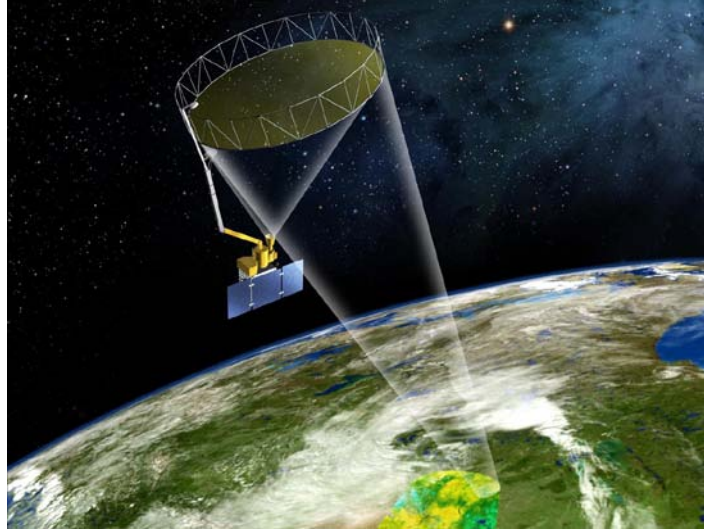


Figure 1. The SMAP observatory is a dedicated spacecraft with a rotating 6-m light-weight deployable mesh reflector. The radar and radiometer share a common feed.

To obtain the desired high spatial resolution the radar employs range and Doppler discrimination. The radar data can be processed to yield resolution enhancement to 1-3 km spatial resolution over the 70% outer parts of the 1000 km swath. Data volume prohibits the downlink of the entire radar data acquisition. Radar measurements that allow high-resolution processing will be collected during the morning overpass over all land regions and extending one swath width over the surrounding oceans. During the evening overpass data poleward of 45° N will be collected and processed as well to support robust detection of landscape freeze/thaw transitions.

The baseline orbit parameters are:

- Orbit Altitude: 685 km (2-3 days average revisit and 8-days exact repeat)
- Inclination: 98 degrees, sun-synchronous
- Local Time of Ascending Node: 6 pm

At L-band anthropogenic Radio Frequency Interference (RFI), principally from ground-based surveillance radars, can contaminate both radar and radiometer measurements. Early measurements and results from the SMOS mission indicate that in some regions RFI is present and detectable. The SMAP radar and radiometer electronics and algorithms have been designed to include features to mitigate the effects of RFI. To combat this, the SMAP radar utilizes selective filters and an adjustable carrier frequency in order to tune to pre-determined RFI-free portions of the spectrum while on orbit. The SMAP radiometer will implement a combination of time and frequency diversity, kurtosis detection, and use of T_4 thresholds to detect and where possible mitigate RFI.

The SMAP L1-L4 data products are listed in Table 2. Level 1B and 1C data products are calibrated and geolocated instrument measurements of surface radar backscatter cross-section and brightness temperatures derived from antenna temperatures. Level 2 products are geophysical retrievals of soil moisture on a fixed Earth grid based on Level 1 products and

ancillary information; the Level 2 products are output on half-orbit basis. Level 3 products are daily composites of Level 2 surface soil moisture and freeze/thaw state data. Level 4 products are model-derived value-added data products that support key SMAP applications and more directly address the driving science questions.

Table 2. SMAP Data Products

Product	Description	Gridding (Resolution)	Latency	
L1A_TB	Radiometer Data in Time-Order	-	12 hrs	Instrument Data
L1A_S0	Radar Data in Time-Order	-	12 hrs	
L1B_TB	Radiometer T_{β} in Time-Order	(36x47 km)	12 hrs	
L1B_S0_LoRes	Low Resolution Radar σ_0 in Time-Order	(5x30 km)	12 hrs	
L1C_S0_HiRes	High Resolution Radar σ_0 in Half-Orbits	1 km (1-3 km)	12 hrs	
L1C_TB	Radiometer T_{β} in Half-Orbits	36 km	12 hrs	
L2_SM_A	Soil Moisture (Radar)	3 km	24 hrs	Science Data (Half-Orbit)
L2_SM_P	Soil Moisture (Radiometer)	36 km	24 hrs	
L2_SM_AP	Soil Moisture (Radar + Radiometer)	9 km	24 hrs	
L3_FT_A	Freeze/Thaw State (Radar)	3 km	50 hrs	Science Data (Daily Composite)
L3_SM_A	Soil Moisture (Radar)	3 km	50 hrs	
L3_SM_P	Soil Moisture (Radiometer)	36 km	50 hrs	
L3_SM_AP	Soil Moisture (Radar + Radiometer)	9 km	50 hrs	
L4_SM	Soil Moisture (Surface and Root Zone)	9 km	7 days	Science Value-Added
L4_C	Carbon Net Ecosystem Exchange (NEE)	9 km	14 days	

1.2 SMAP REQUIREMENTS RELATED TO FREEZE/THAW STATE

The primary science objectives for SMAP directly relevant to the freeze/thaw measurement include linking terrestrial water, energy and carbon cycle processes, quantifying the net carbon flux in boreal landscapes and reducing uncertainties regarding the so-called missing carbon sink on land. This leads to the following requirements on the freeze/thaw measurement:

- 1) *surface freeze/thaw measurements shall be provided over land areas where these factors are primary environmental controls on land-atmosphere exchanges of water, energy and carbon;*
- 2) *the freeze/thaw status of the aggregate vegetation-soil layer shall be determined sufficiently to characterize the low-temperature constraint on vegetation net primary productivity and surface-atmosphere CO₂ exchange;*
- 3) *SMAP shall measure landscape freeze/thaw with a spatial resolution of 3 km;*

- 4) *SMAP shall measure landscape freeze/thaw with a mean temporal sampling of 2 days or better;*
- 5) *SMAP shall measure freeze/thaw with accuracy sufficient to resolve the temporal dynamics of net ecosystem exchange to within 0.05 tons C ha⁻¹ (or 3%) over a ~100-day growing season.*

Current SMAP baseline mission requirements specific to terrestrial freeze/thaw science activities state that:

[Level 1 mission requirement] The baseline science mission shall provide estimates of surface binary freeze/thaw state for the region north of 45° N latitude, which includes the boreal forest zone, with a spatial classification accuracy of 80% at 3 km spatial resolution and 2-day average intervals.

The above requirements form the basis of the design of the L3_FT_A product. This document includes a description of the baseline freeze/thaw state classification algorithm, and discussion of theoretical assumptions and procedures for refining and testing the algorithm to achieve the mission requirement.

2 BACKGROUND AND HISTORICAL PERSPECTIVE

The terrestrial cryosphere comprises cold areas of Earth's land surface where water is either permanently or seasonally frozen. This includes most regions north of 45°N latitude and most areas with elevation greater than 1000 meters. Within the terrestrial cryosphere, spatial patterns and timing of landscape freeze/thaw state transitions are highly variable with measurable impacts to climate, hydrological, ecological and biogeochemical processes.

Landscape freeze/thaw state influences the seasonal amplitude and partitioning of surface energy exchange strongly, with major consequences for atmospheric profile development and regional weather patterns (Betts et al., 2000). In seasonally frozen environments, ecosystem responses to seasonal thaw are rapid, with soil respiration and plant photosynthetic activity accelerating with warmer temperatures and the abundance of liquid water (e.g., Goulden et al., 1998; Black et al., 2000; Jarvis and Linder, 2000). The timing of seasonal freeze/thaw transitions can generally be related to the duration of seasonal snow cover, frozen soils, and the timing of lake and river ice breakup and flooding in the spring (Kimball et al., 2001, 2004a). The seasonal non-frozen period also bounds the vegetation growing season, while annual variability in freeze/thaw timing has a direct impact on net primary production and net ecosystem CO₂ exchange (NEE) with the atmosphere (Vaganov et al., 1999; Goulden et al., 1998).

Satellite-borne microwave remote sensing has unique capabilities that allow near real-time monitoring of freeze/thaw state, without many of the limitations of optical-infrared sensors such as solar illumination or atmospheric conditions. The SMAP L3_FT_A product is designed to provide the most accurate remote sensing-based characterization of landscape freeze/thaw state for land areas north of 45°N latitude. The unique design of the SMAP L-band radar allows a

combined spatial and temporal characterization of terrestrial freeze/thaw transitions previously unavailable.

The SMAP L3_FT_A baseline algorithm follows from an extensive heritage of previous work, initially involving truck mounted radar scatterometer and radiometer studies over bare soils and croplands (Ulaby et al., 1986; Wegmuller, 1990), followed by aircraft SAR campaigns over boreal landscapes (Way et al., 1990), and subsequently from a variety of satellite-based SAR, radiometer, and scatterometer studies at regional, continental and global scales (Rignot and Way, 1994; Rignot et al., 1994; Way et al., 1997; Frohling et al., 1999; Wisman, 2000; Kimball et al., 2001; 2004a,b; McDonald et al., 2004; Rawlins et al., 2005; Du et al. 2014; Podest et al. 2014; Kim et al. 2014a). These investigations have included regional, pan-boreal, and global scale efforts, supporting development of retrieval algorithms, assessment of applications of remotely sensed freeze/thaw state for supporting ecologic and hydrological studies, and more recently in assembly of a global-scale Earth System Data Record (ESDR) developed from higher frequency (37 GHz) overlapping SMMR, SSM/I and AMSR-E sensor records, and distributed through the National Snow and Ice Center (Kim, et al., 2011; 2012). The global freeze/thaw ESDR is the first of its kind, providing daily freeze/thaw state across multiple decades and including delineation of AM/PM freeze/thaw transitional states.

The SMAP L3_FT_A algorithm classifies the land surface freeze/thaw state based on the time series of L-band radar backscatter response to the change in dielectric constant of the land surface components associated with water transitioning between solid and liquid phases. The lower frequency (L-band) radar backscatter measurements from SMAP will provide enhanced sensitivity to freeze/thaw conditions in vegetation canopy, snow and surface soil layers, while the relative radar penetration depth and sensitivity of the freeze/thaw signal to these landscape elements is expected to vary according to surface moisture and vegetation biomass conditions, and underlying land cover and terrain heterogeneity (Podest et al. 2014; Du et al. 2014). The freeze/thaw signal dominates the seasonal pattern of radar backscatter for regions of the global land surface undergoing seasonal freeze/thaw transitions. The timing of the springtime freeze/thaw state transitions corresponding to this radar backscatter response coincides with the timing of growing season initiation in boreal, alpine and arctic tundra regions of the global cryosphere. Interannual variability in these processes is a major control on annual vegetation productivity and land-atmosphere CO₂ exchange (Frohling et al., 1999; Kimball et al., 2004; McDonald et al., 2004). Thus the L3_FT_A algorithm supports characterization of the spatial and temporal dynamics of landscape freeze/thaw state for regions of the global land surface where (1) cold temperatures are limiting for photosynthesis and respiration processes, (2) the timing and variability in landscape freeze/thaw processes have a key impact on vegetation productivity and the carbon cycle, and (3) the thermal state of the soil has a strong influence on surface hydrological processes.

2.1 PRODUCT/ALGORITHM OBJECTIVES

Figure 2 shows the data sets and processing chain associated with SMAP freeze/thaw algorithm implementation and product generation, including input and output data. There is one primary SMAP freeze/thaw product, L3_FT_A, which consists of daily composite landscape freeze/thaw state derived from the AM (descending) and PM (ascending) overpass radar data

(L1C_S0_HiRes half-orbits) north of 45°N. The L1C_S0_HiRes AM data will also be utilized to generate a freeze/thaw binary state flag for use in the L2/3_SM product algorithms that is not constrained by the 45°N coverage limit of the PM overpass SAR retrievals. The L3_FT_A product is gridded and provided on a 3 km Equal Area Scalable Earth grid version 2 (EASE-grid) in both global and north polar projections.

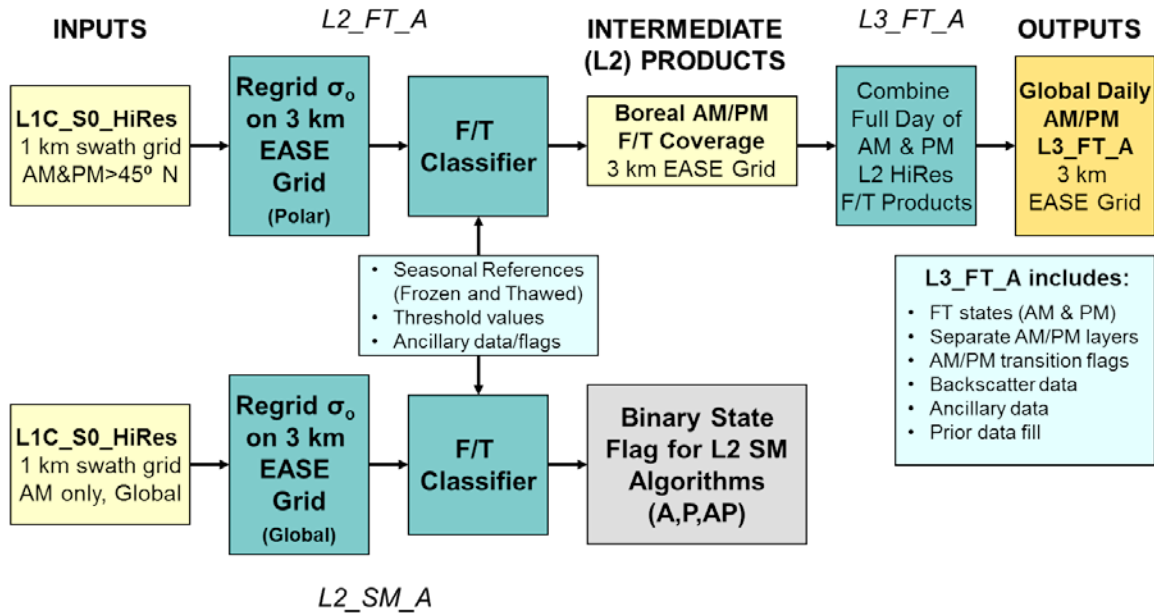


Figure 2. Processing sequence for generation of the L3_FT_A product and the binary freeze/thaw state flag to be used in generation of the SMAP soil moisture products.

The baseline L3_FT_A product is designed to fulfill the SMAP mission freeze/thaw science requirements summarized in Section 1 above. The baseline product provides freeze/thaw state classification information at a spatial resolution of 3 km with temporal revisit of 2 days or better north of ~55°N and 3 days or better north of 45°N. The freeze/thaw classification domain covers regions of Earth’s land mass where low temperatures are a significant constraint to vegetation productivity and terrestrial carbon exchange (Churkina and Running, 2000; Nemani et al., 2003; Kim et al., 2011). Product accuracy associated with meeting SMAP mission requirements will focus solely on the product domain north of 45°N latitude.

Freeze/thaw state will be generated separately for AM and PM radar acquisitions (upper processing chain noted under ‘L2_FT_A’ in Figure 2). Combining SMAP freeze/thaw state assessments from AM and PM acquisitions for the L3_FT_A product provides information on regions undergoing freeze/thaw transitions on a diurnal basis (e.g. Kim et al., 2011). This aspect of the product supports enhanced investigation of spring and autumn transition seasons and the associated controls on annual vegetation productivity (e.g. Kim et al. 2012).

The radar freeze/thaw algorithm will also supply a 3 km resolution AM global binary freeze/thaw state flag as an intermediate output product to be utilized within the L2_SM_A radar

soil moisture processing to identify frozen land regions, and in that context supporting the generation of the L2 and L3 active, passive, and active-passive products (L2/3_SM_A, L2/3_SM_P, L2/3_SM_AP; lower processing chain noted above ‘L2_SM_A’ in Figure 2). Accuracy of the AM overpass freeze/thaw estimates including regions south of 45°N, which will feed into other SMAP products, will be assessed as part of SMAP L4 product cal/val activities.

The 45°N latitude limit for L1C_S0_HiRes coverage for both AM and PM orbits, and hence the ability to derive the daily L3_FT_A product, has a physical basis in the magnitude of the difference between the thawed and frozen radar reference values that are a key component of the retrieval (see section 4.1.1). Reference value differences below approximately 1.5 dB will limit the ability to distinguish frozen versus thawed ground from the radar signal and significantly increase freeze/thaw retrieval uncertainty. The difference in reference values (thawed – frozen) derived from Aquarius L-band radar scatterometer measurements is shown in Figure 3. The 45°N latitude limit approximates the transition from reference differences which exceed 3 dB to reference differences near 0 dB.

There is also a climatological motivation to imposing a latitudinal limit on the L3_FT_A product. Freeze events, particularly in non-alpine regions, tend to be ephemeral below approximately 45°N (which also explains the weak reference scene differences in Figure 3). As shown in Figure 4, there is widespread positive correspondence between variability in the length of the non-frozen season (derived from SSM/I 37 GHz brightness temperatures) and NDVI summer growth changes (derived from the MODIS MOD13 NDVI record) over northern (>=45°N) land areas, consistent with frozen season constraints on vegetation productivity over the northern domain (Kim et al., 2012). The relative influence of freeze/thaw and non-frozen season effects on vegetation growth is less widespread at lower latitudes due to a general reduction of cold temperature constraints to productivity and a relative increase in other environmental controls such as moisture limitations (e.g. Kim et al. 2014a).

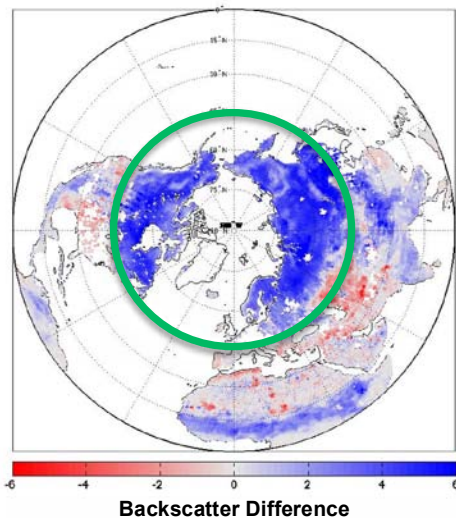


Figure 3. Reference backscatter difference (thawed – frozen) derived from Aquarius measurements (2012-2013). Thawed (frozen) reference represents the mean of the 10 highest (lowest) backscatter values from July and August (January and February). Green circle indicates 45°N latitude.

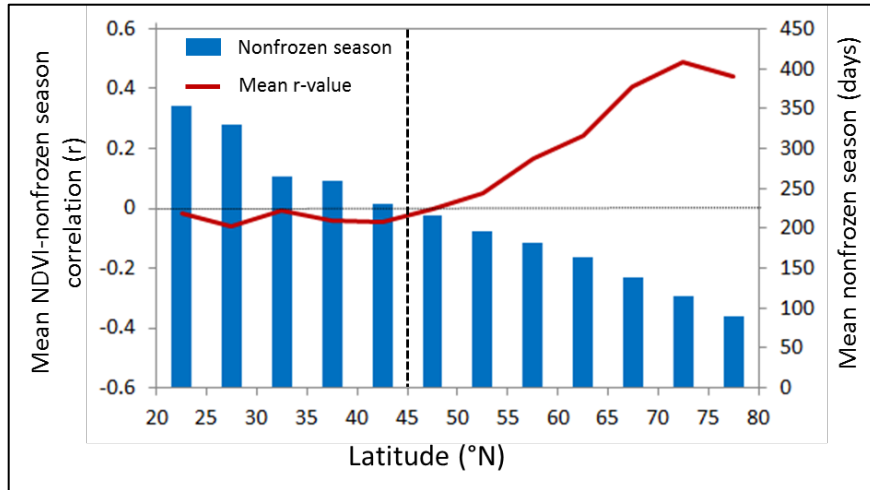


Figure 4. Latitudinal variation in mean correlations (r) between annual non-frozen season variations and summer (JJA) NDVI growth anomalies defined over a 9-year record (2000-2008) (after Kim et al. 2012, Fig 5b).

2.2 L3_FT_A PRODUCTION

Production of the L3_FT_A data sets will be carried out at JPL during SMAP mission operations. An overview of the L3_FT_A processing sequence is provided in Figure 2. Research using SSM/I radiometer and SeaWinds-on-QuikSCAT scatterometer data indicate substantial variability of freeze/thaw spatial and temporal dynamics derived from AM and PM overpass data with important linkages to surface energy balance and carbon cycle dynamics (McDonald and Kimball, 2005; Kim et al., 2011). L3_FT_A algorithm products generated utilizing both ascending (PM) and descending (AM) radar backscatter data streams will enable regional assessment and monitoring of diurnal variability in terrestrial freeze/thaw state dynamics.

SMAP mission specifications provide for collection of high resolution (3 km) radar backscatter (L1C_S0_HiRes) for descending orbits (6 AM overpass) over land and for that portion of ascending orbits (6 PM overpass) over land north of 45°N latitude. Low (~5x30 km) resolution radar data (L1B_S0_LoRes) provides global coverage for AM and PM overpass orbits. These radar backscatter data streams will provide calibrated and geolocated σ_0 data, with L1B_S0_LoRes in time order and L1C_S0_HiRes in individual half-orbit files. The L3_FT_A product will utilize the L1C_S0_HiRes data stream for standard production.

The L3_FT_A algorithm will be applied to the radar data granules for unmasked land regions. The resulting intermediate freeze/thaw products (Figure 2) will serve two purposes: (1) these data will be assembled into global daily composites in production of the L3_FT_A product, and (2) the freeze/thaw product derived from global AM L1C_S0_HiRes granules will provide the binary freeze/thaw state flag supporting generation of the L2 and L3 soil moisture products.

The L3_FT_A algorithm is applied to the total power radar data streams, total power being the sum of HH, VV, and HV polarized backscatter. This will provide the best signal-to-noise characteristic from the SMAP radar, thus optimizing product accuracy. The L3_FT_A algorithms

may also be employed to produce landscape freeze/thaw state information from SMAP L1C_TB brightness temperature observations. Hence in the event of a failure of the SMAP radar data stream, freeze/thaw data products could be produced using the L1C_TB data stream, but at the coarser spatial resolution (36 km) of the L1C_TB product. Research and development on passive only algorithms using SMOS and Aquarius measurements are ongoing outside of formal SMAP activities (for example, Rautiainen et al., 2014).

No L3_FT_A data processing will occur over masked areas. The freeze/thaw retrieval will take into account the transient open water flag determined from the 3 km gridded backscatter in the L2_SM_A processing. It is anticipated that “no-data” flags will be associated with the L3_FT_A product identifying each of the masked surface types: ocean and inland open water (static and transient), permanent ice and snow, and urban areas. The L3_FT_A algorithms do not utilize ancillary data during execution and processing, however, ancillary data will be utilized to optimize the state change thresholds that are employed in the baseline algorithm scheme (see section 4.2.3). Although not strictly required, prior initialization of these thresholds enhances algorithm efficiency and accuracy. Ancillary data planned for use in generation of the L3_FT_A product are summarized in Section 4.2.2.

2.3 DATA PRODUCT CHARACTERISTICS

The L3_FT_A product will delineate freeze/thaw state on a pixel-wise basis according to the nomenclature in Table 4. An example of this product derived from Aquarius radar measurements utilizing the baseline L3_FT_A algorithm and domain is shown in Figure 3.

Table 3. Nomenclature of the SMAP L3_FT_A product, indicating the landscape state as observed during AM and PM overpasses, and the corresponding freeze/thaw classification terminology.

Landscape State		F/T Classification
AM Overpass	PM Overpass	Terminology combining AM and PM data
Frozen	Frozen	Frozen
Thawed	Thawed	Thawed
Frozen	Thawed	Transitional
Thawed	Frozen	Inverse-Transitional

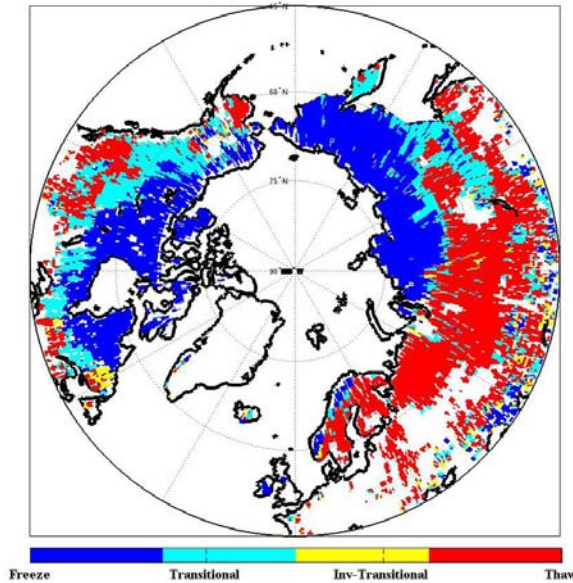


Figure 3. Example of a global daily freeze/thaw product for April 15, 2014 derived from Aquarius backscatter measurements. Regions of frozen, thawed, transitional, and inverse-transitional are identified.

Radar backscatter observations are acquired for the global land surface at 3 km resolution (L1C_S0_HiRes) for the AM (descending) orbital nodes. For the PM (ascending) orbital nodes, high-resolution backscatter (L1C_S0_HiRes) is acquired at 3 km resolution for regions north of 45°N latitude. Low-resolution radar (L1B_S0_LoRes) data at 5x30 km will be available for regions south of 45°N latitude on the PM passes but are not utilized for any FT product generation. The L3_FT_A product will use both AM and PM high resolution data in combination to delineate frozen, thawed, transitional and inverse transitional conditions for unmasked land areas north of 45°N. All renderings are posted to a 3 km EASE-Grid, both in global and north polar projections.

The L3_FT_A algorithm will be applied to regridded L1C_S0_HiRes radar data as a baseline (Figure 2). Implementing the L3_FT_A algorithm in this way will ensure production of the binary state freeze/thaw flag consistent with the needs of the L2/L3 soil moisture processing. The intermediate orbit-specific freeze/thaw products will be temporally composited to assemble freeze/thaw state maps separately for AM and PM acquisitions. The daily temporal compositing process will be performed on the 3 km EASE grid data, retaining the freeze/thaw state associated with those acquisitions closest to 6:00 AM local time (AM daily product) and 6:00 PM local time (PM daily product). These intermediate products will be further composited into the daily L3_FT_A product, keeping the latest date of acquisition as a replacement for acquisitions acquired on older dates, to ensure full coverage of the freeze/thaw domain from AM and PM acquisitions separately. These AM and PM multi-date composites will be used to derive the combined product with nomenclature shown in Table 3 above. The respective date and time of acquisition of each of the AM and PM components of the data stream will be maintained in the data set. The daily L3_FT_A product will thus incorporate AM and PM data for the current day, as well as past days' information (to a maximum of 3 days, necessary only near the southern

margin of the FT domain) to ensure complete coverage of the freeze/thaw domain in each day's product.

Formatting of the L3_FT_A product will be HDF5 with appropriate metadata. The L3_FT_A will be posted to both polar and global equal-area Earth grids. The projections are defined in terms of north polar azimuthal and global cylindrical Equal-Area Scalable Earth (EASE; version 2) grids (Armstrong and Brodzik, 1995). These gridding schemes are similar to current versions of the SSM/I derived FT ESDR (<http://nsidc.org/data/NSIDC-0477>).

Latency is defined as the average time under normal operating conditions between data acquisition by the SMAP observatory and delivery of the product to the data center. Latency of the baseline L3_FT_A product is dependent on the delivery rate of L1C_S0_HiRes (47 GB per day) data from the radar processing system and on the rate at which these can be processed into freeze/thaw products and submitted to the SMAP NSIDC DAAC. Processing of the baseline L3_FT_A product will be complete within 24 hours of receipt of the global L1C_S0_HiRes data, which itself has a latency of 12 hours.

3 PHYSICS OF THE PROBLEM

3.1 SYSTEM MODEL

The ability of microwave remote sensing instruments to observe freezing and thawing of a landscape has its origin in the distinct changes of surface dielectric properties that occur as water transitions between solid and liquid phases. A material's permittivity describes how that material responds in the presence of an electromagnetic field (Kraszewski, 1996). As an electromagnetic field interacts with a dielectric material, the resulting displacement of charged particles from their equilibrium positions gives rise to induced dipoles that respond to the applied field. A material's permittivity is a complex quantity (*i.e.*, having both real [ϵ'] and imaginary [ϵ''] numerical components) expressed as:

$$\epsilon = \epsilon' - j\epsilon'' \quad (1)$$

and is often normalized to the permittivity of a vacuum (ϵ_0) and referred to as the relative permittivity, or the *complex dielectric constant*:

$$\epsilon_r = \epsilon' / \epsilon_0 - j\epsilon'' / \epsilon_0 = \epsilon_r' - j\epsilon_r'' \quad (2)$$

The real component of the dielectric constant, ϵ_r' , is related to a material's ability to store electric field energy. The imaginary component of the dielectric constant, ϵ_r'' , is related to the dissipation or energy loss within the material. At microwave wavelengths, the dominant phenomenon contributing to ϵ_r'' is the polarization of molecules arising from their orientation with the applied field. The dissipation factor, or *loss tangent*, is defined as the ratio:

$$\tan(\delta) = \epsilon_r'' / \epsilon_r' \quad (3)$$

Consisting of highly polar molecules, liquid water exhibits a dielectric constant that dominates the microwave dielectric response of natural landscapes (Ulaby *et al.*, 1986). As liquid water

freezes, the molecules become bound in a crystalline lattice, impeding the free rotation of the polar molecules and reducing the dielectric constant substantially. In general, landscapes of the terrestrial cryosphere consist of a soil substrate that may be covered by some combination of vegetation and seasonal or permanent snow. The sensitivity of radar and brightness temperature signatures to these landscape features is affected strongly by the sensing wavelength, as well as landscape structure and moisture conditions. The composite remote sensing signature represents a sampling of the aggregate landscape dielectric and structural characteristics, with sensor wavelength having a strong influence on the sensitivity of the remotely sensed signature to the various landscape constituents.

3.2 RADIATIVE TRANSFER AND BACKSCATTER

In the microwave region of the electromagnetic spectrum, vegetation canopies may be considered to be weakly scattering media (*i.e.* media characterized by volume absorption that is much larger than volume scattering), with the first-order approximation to canopy scattering being applicable. In this case, diffuse scattering effects may be ignored and first-order scattering model approaches utilized to interpret backscatter (Ulaby *et al.*, 1986). At higher frequencies, scattering effects of the vegetation are increasingly significant. The dependence of the microwave signatures on vegetation characteristics is complex, with vegetation structure strongly influencing radar signatures.

Radar remote sensing of the total co-polarized backscatter from the landscape at polarization p is the sum of three components:

$$\sigma_{pp}^t = \sigma_{pp}^s \exp(-2\tau_c) + \sigma_{pp}^{vol} + \sigma_{pp}^{int} \quad (4)$$

The first term is the surface backscatter, σ_{pp}^s , modified by the two-way attenuation through a vegetation layer of opacity τ_c along the slant path. The second term represents the backscatter from the vegetation volume, σ_{pp}^{vol} . The third term represents interactions between vegetation and the surface, σ_{pp}^{int} (Ulaby *et al.*, 1986; Ulaby *et al.*, 1990; Kuga *et al.*, 1990).

The response of σ_{pp}^t to freeze/thaw dynamics is affected by surface roughness, topography, vegetation, and snow cover. The relative contribution of the three terms in Equation (4) is influenced by the canopy opacity, τ_c . Opacity and volume scattering vary significantly with frequency. For bare surfaces or sparsely vegetated conditions, the surface terms dominate the received signal, with σ_{pp}^t being influenced primarily by contributions from the soil surface and snow cover. Because of the high dielectric constant of liquid water, microwave penetration of the vegetation decreases as biomass moisture levels increase. In general, τ_c increases with increasing frequency, vegetation density, and dielectric constant. High frequency, short wavelength energy (*e.g.* Ku-band) has higher τ_c and does not penetrate as significantly into vegetation canopies as

lower frequency, longer wavelength energy (e.g. L-band). Hence, lower frequency sensors are generally more sensitive to properties of surfaces underlying dense vegetation canopies. However, the dependence of σ_{pp}^f on snow characteristics is also complex, with snow pack wetness, density, crystal structure, and depth influencing backscatter. The effect of snow cover on radar backscatter is more significant at higher frequencies owing to the increased scattering albedo of the snow pack at short wavelengths relative to longer wavelengths (e.g., Ulaby *et al.*, 1986; Raney, 1998) These phenomena lead to notable differences in the temporal response of emission and backscatter to landscape freeze/thaw processes with sensor wavelengths (e.g., Way *et al.*, 1994; Way *et al.*, 1997; Frohling *et al.*, 1999; Kimball *et al.*, 2001; Du *et al.*, 2014).

4 RETRIEVAL ALGORITHM

4.1 THEORETICAL DESCRIPTION

Derivation of the SMAP L3_FT_A product will employ a temporal change detection approach that has been previously developed and successfully applied using time-series satellite remote sensing radar backscatter and radiometric brightness temperature data from a variety of sensors and spectral wavelengths. The approach is to identify landscape freeze/thaw transition by identifying the temporal response of radar backscatter to changes in the dielectric constant of the landscape components that occur as the water within the components transitions between frozen and non-frozen conditions. Classification algorithms assume that the large changes in dielectric constant occurring between frozen and non-frozen conditions dominate the corresponding backscatter temporal dynamics across the seasons, rather than other potential sources of temporal variability such as changes in canopy structure and biomass or large precipitation events. This assumption is valid for most areas of the terrestrial cryosphere.

4.1.1 BASELINE ALGORITHM: SEASONAL THRESHOLD APPROACH

The SMAP freeze/thaw algorithm is based on a seasonal threshold approach. While other freeze/thaw algorithmic approaches are possible (for example, moving window; temporal edge detection) these techniques do not fulfill the SMAP data latency requirement, and so are not discussed further in this document.

The seasonal threshold (baseline) algorithm examines the time series progression of the remote sensing signature relative to signatures acquired during seasonal reference frozen and thawed states. This algorithm is well-suited for application to data with temporally sparse or variable repeat-visit observation intervals and has been applied to ERS and JERS Synthetic Aperture Radar (SAR) imagery (e.g. Rignot and Way, 1994; Way *et al.*, 1997; Gamon *et al.*, 2004; Entekhabi *et al.*, 2004; Podest *et al.* 2014). A seasonal scale factor $\Delta(t)$ may be defined for an observation acquired at time t as:

$$\Delta(t) = \frac{\sigma(t) - \sigma_{fr}}{\sigma_{th} - \sigma_{fr}} \quad (5)$$

where $\sigma(t)$ is the measurement acquired at time t , for which a freeze/thaw classification is sought, and σ_{fr} and σ_{th} are backscatter measurements corresponding to the frozen and thawed reference states, respectively. A major component of the SMAP baseline algorithm development involved application of existing satellite L-band radar measurements from the Aquarius mission over the FT domain to develop pre-launch maps of σ_{th} , and σ_{fr} . These initial references will be replaced through post-launch integration of references derived from SMAP measurements (Section 4.2.3).

A threshold level T is then defined such that:

$$\begin{aligned} \Delta(t) &> T \\ \Delta(t) &\leq T \end{aligned} \tag{6}$$

defines the thawed and frozen landscape states, respectively. This series of algorithms will be run on a cell-by-cell basis for unmasked portions of the FT domain. The output from Equation (6) will be a dimensionless binary state variable designating either frozen or thawed condition for each unmasked grid cell.

The parameter T will be fixed at 0.5 at the start of the SMAP mission, but can be optimized for various land cover and soil conditions. Optimizing of T will occur only after the SMAP reference values are updated from the pre-launch Aquarius derived values to actual SMAP references (see Section. 4.2.3).

4.1.2 VARIANCE AND UNCERTAINTY ESTIMATES

Primary sources of error and uncertainty in the freeze/thaw product stems from: (1) radiometric errors due to resolution and sensor viewing geometry (azimuth), (2) geometric errors due to layover and shadowing (slope/aspect), (3) within-season radar backscatter variability not accounted for by the implementation of constant frozen and thawed reference states employed within the baseline algorithm, (4) variations in landcover with respect to spatial heterogeneity, (5) the presence of a thick organic layer overlying mineral soil which can retain liquid water for prolonged periods in winter, and (6) uncertainties related to wet snow cover. Some additional sources are associated with relatively dry landscapes that contain small amounts of water such that changes in freeze/thaw state result in minimal change in backscatter. Large precipitation events that significantly wet the land surface such that the additional surface water induces a pronounced backscatter change may induce an error in the classified freeze/thaw state.

High resolution PALSAR measurements over Alaska were utilized pre-launch to evaluate the suitability of coarse resolution Aquarius data to provide useful hemispheric scale reference states for the initial SMAP freeze/thaw algorithm. Post-launch assessment of SMAP measurements will be made using PALSAR-2 data sets to assist in the error and uncertainty assessment of system level parameters (e.g. system noise, viewing geometry, and associated topographic effects).

The classification accuracy of freeze/thaw state was simulated using the expected SMAP system noise vs. the difference in backscatter between the thawed and frozen states (Figure 4). A

step size of at least 1.5 dB will meet the classification accuracy of 80%, calculated on an annual basis.

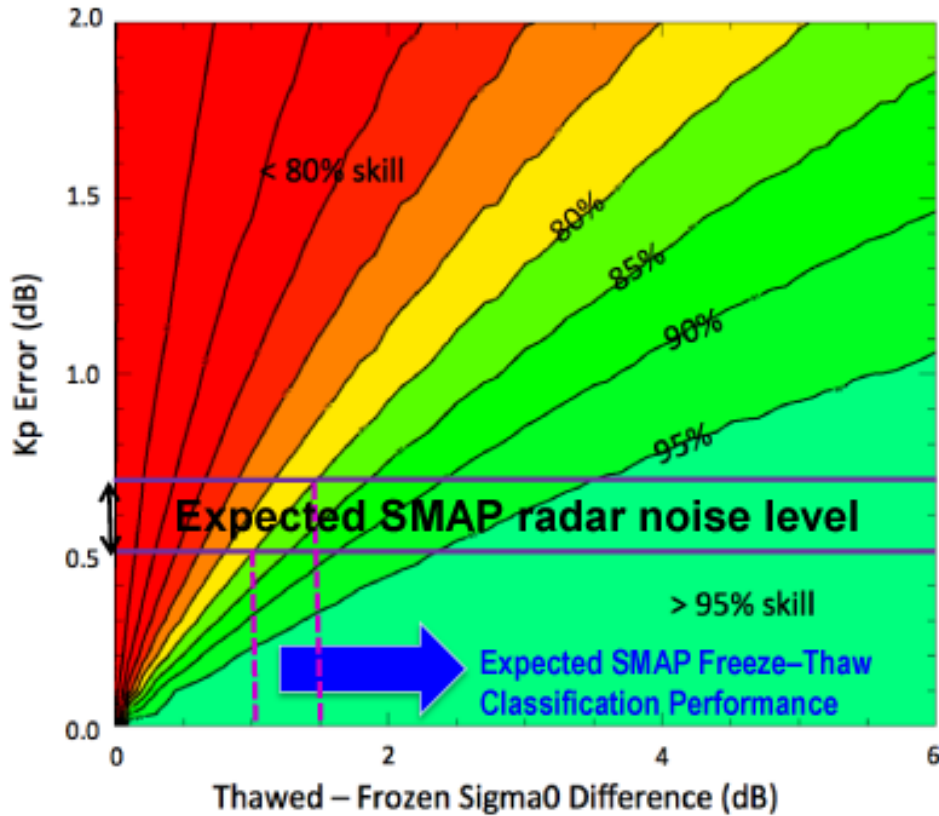


Figure 4. Simulation of classification accuracy versus radar noise and freeze/thaw state step size in backscatter. The required accuracy or skill is 80%.

The sensitivity of the SMAP L-band backscatter response to variations in vegetation structure and biomass, fractional open water, snow cover, and topographic slope and aspect will be assessed. Trade-offs between satellite data acquisition timing (e.g., AM and PM overpass and temporal compositing), polarization (e.g., total power vs. single/cross polarization) and sensitivity to freeze/thaw and terrestrial carbon cycle processes will also be evaluated in the context of the L4_C requirements. Verification of methods will include intercomparisons among radar backscatter and ecological process model simulations over existing biophysical station networks. These efforts will be coordinated with the SMAP L4 Carbon (L4_C) product activities.

4.2 PRACTICAL CONSIDERATIONS

4.2.1 PROCESSING AND DATA FLOW CONSIDERATIONS

Freeze/thaw state flags are required for the Level 2 soil moisture processing (active, passive, and active-passive). The L3_FT_A processing algorithm is implemented in the L2_SM_A as part of a “front-end” executable which performs the backscatter regridding, radar vegetation index (RVI) computation, transient water body detection, and freeze/thaw state retrieval, in order to provide these flags for the subsequent soil moisture retrievals. This front-end generates a temporary file for each pass containing the gridded backscatter and flags. This temporary file (which is also directly appended to the L2_SM_A product) can be used directly by the L3_FT_A processing to generate the daily grid of the freeze/thaw states derived from the high-resolution radar.

4.2.2 ANCILLARY DATA AVAILABILITY/CONTINUITY

Ancillary datasets will be used to (1) support initialization of the references and updating of the thresholds employed in the algorithm, (2) set flags that indicate potential problem regions, and (3) define masks where no retrievals should be performed. Ancillary datasets of inland open water, permanent ice and snow, and urban areas will be used to derive masks so that no retrievals occur over these regions. Ancillary datasets of mountainous areas, fractional open water cover, and precipitation will be used to derive flags so that a confidence interval can be associated with the retrieval. A primary source for each of the above ancillary parameters has been selected. These data are common to all algorithms using that specific parameter. All ancillary datasets will be resampled to a spatial scale and geographic projection that matches the L3_FT_A product in accordance with the guidelines of the SMAP ADT/SDT/ST. These data will be archived in a shared master file of ancillary data to ensure consistency across the SMAP data processing and algorithm product array.

Ancillary datasets used for L3_FT_A data processing will be in place prior to launch, without the need for periodic updates during post-launch operations. A continuous surface map of fractional area of open water will be used to represent fractional water coverage within a grid consistent with the resolution and projection of the L3_FT_A product. This information will then be used for developing an open water mask for the domain. We will conduct investigations to set a minimum open water threshold for masking grid cells. The mask will be used for screening radar data prior to application of the freeze/thaw algorithms. The mask will be applied to the regridded L1C_S0_HiRes data stream prior to application of the freeze/thaw algorithms. No further freeze/thaw data processing will occur for grid cells within masked regions. Table 4 lists the ancillary data to be employed in support of the L3_FT_A product. Ancillary data sets are described in separate documents for each data set.

Table 4. Input datasets needed for generation of the L3_FT_A

Data Type	Data Source	Frequency	Resolution	Extent	Use
Vegetation type	MODIS-IGBP	Once	250 m	Global	Sensitivity Analysis
Land Surface Temperature	MERRA and station data	Daily or close to time of acquisition	25 km and point data	Global	Algorithm Parameterization
Precipitation	ECMWF forecasts	Time of acquisition	0.25 degrees	Global	Sensitivity Analysis
Static Water bodies	MODIS44W	Once	250 m	Global	Mask/Flag
Transient Water Bodies	SMAP L2_SM_A	As processed	3 km	Global	Mask/Flag
Mountainous Areas	NASA Global DEM	Once	30 m	Global	Mask/Flag
Permanent Ice and Snow	MODIS-IGBP permanent ice and snow class	Once	500 m	Global	Mask/Flag
Seasonal Snow	NOAA IMS	Daily	1 km	Northern Hemisphere	Flag
Urban Areas	Global Urban Mapping Project (GRUMP)	Once	1 km	Global	Mask/Flag

4.2.3 UPDATING AND OPTIMIZATION OF REFERENCES AND THRESHOLDS

Pre-launch freeze and thaw thresholds were determined using weekly L-band radar measurements from the Aquarius mission. Land-only swath measurements were binned to the 36 km EASE-Grid, using a normalized incidence angle of 40 degrees (combined from the three Aquarius beams). Data were separated by ascending and descending orbit. Various techniques were tested for isolating measurements characteristic of frozen and thawed conditions, including temporal averages (i.e. during January/February for freeze; July/August for thaw) and averages of a fixed number of lowest/highest seasonal backscatter values. In the end, the references were determined by averaging the 10 lowest (freeze) and 10 highest (thaw) backscatter measurements from July 2013 through March 2014. This technique may introduce uncertainty near the southern margin of the FT domain where ephemeral freeze events may not produce conditions for 10 representative ‘freeze’ measurements in the coarse spatial and temporal resolution Aquarius dataset, so refinements to the definition of the pre-launch references are ongoing. Gaps due to

radio frequency interference (RFI) in the Aquarius derived references were filled by applying land cover specific averages to grid cells with missing values.

Given the limitations of the Aquarius measurements, it is highly desirable to switch to references derived from SMAP measurements as early in the mission as possible. Overviews of the planned update schedule are provided in Figure 5 and Table 5. Following the in-orbit checkout period, the first potential SMAP freeze reference measurements will not be available until the 2015/16 winter. There will be no prior freeze measurements available for updating the freeze references from Aquarius to SMAP during the 2014/2015 winter. The references during the first thaw transition season immediately after IOC will also be Aquarius derived. Complete SMAP derived references will not be fixed until the 2016 spring thaw transition. The references will continue to be evaluated and updated through the entire mission.

At mission start, the freeze/thaw retrieval threshold (t) will be fixed at 0.5. After each transition season, evaluations at the core validation sites, sparse networks, available retrospective (non near real time) measurements, and GEOS-5 simulations will be used to optimize the threshold values. Collectively, the reference and threshold updating procedures conducted at regular intervals throughout the mission will produce multiple freeze/thaw dataset versions with unique reference and threshold values. This ensemble of retrievals will be statistically assessed to determine retrieval sensitivity to changes in these values, and the resulting spread in freeze/thaw estimates will provide a quantitative metric on retrieval uncertainty.

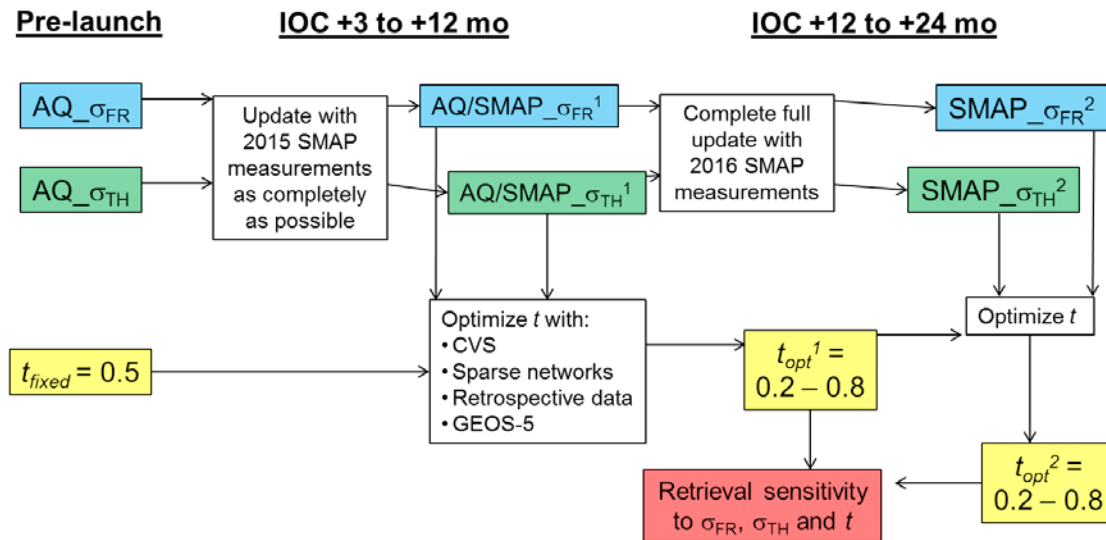


Figure 5. Schedule for updating of freeze/thaw references and optimization of retrieval thresholds during the first two years of the SMAP mission. AQ indicates Aquarius derived references.

Table 5. Schedule for reference updates and threshold optimization. Vertical dashed lines indicate updates which are very close to product delivery milestones.

Activity	2015												2016												2017											
	J	F	M	A	M	J	J	A	S	O	N	D	J	F	M	A	M	J	J	A	S	O	N	D	J	F	M	A	M	J	J	A	S	O	N	D
IOC																																				
Initial L1 release																																				
Validated L1 release																																				
Beta L2-L4 release																																				
Validated L2-L4 release																																				
Key FT transition periods																																				
Updates to σ_{FR} and σ_{TH}																																				
Updates to thresholds																																				

4.2.4 CALIBRATION AND VALIDATION

Accuracy requirements for the L3 freeze/thaw product state that the freeze/thaw status of the aggregate vegetation-soil layer shall be determined sufficiently to characterize the low-temperature constraint on vegetation net primary productivity, and surface-atmosphere CO₂ exchange (see Section 1). Validated science data products shall be made available to the science community starting no later than 12 months after completion of the initial on-orbit checkout period (although it is important to note that the freeze and thaw references may not be fully updated from Aquarius to SMAP derived values by the initial product release – see Section 4.2.3). Selected data products that have not undergone full validation will be made available in near real-time for time-critical applications including processing of the SMAP L3_SM_P data stream, operational forecast demonstrations, and hydrometeorologic and carbon cycle monitoring.

The L3_FT_A freeze/thaw product will provide estimates of land surface freeze/thaw state expressed as a categorical (frozen, thawed, or [inverse]transitional) condition. The SMAP Level 1 mission requirement is that the L3 freeze/thaw product will be provided for land areas north of 45 degrees north latitude with a mean spatial classification accuracy of 80% at 3 km spatial resolution and 2-day average temporal sampling. The accuracy of the L3 product will be determined by comparison of the SMAP freeze/thaw observations with in situ measurements from sites within northern latitude ($\geq 45^\circ N$) land areas (Figure 6). The in situ validation data will include all core validation sites and selected sites from the sparse networks using criteria based on site representativeness (uniform and representative terrain and land cover) consistent with the overlying 3-km resolution satellite retrieval. The validation will be based on reference freeze/thaw flags derived from co-located temperature and soil moisture measurements corresponding to the local time of the descending and ascending satellite overpasses. The soil moisture and soil temperature criteria for the reference flag will be variable depending on soil and land cover conditions, and will be finalized prior to launch using historical data from each site.

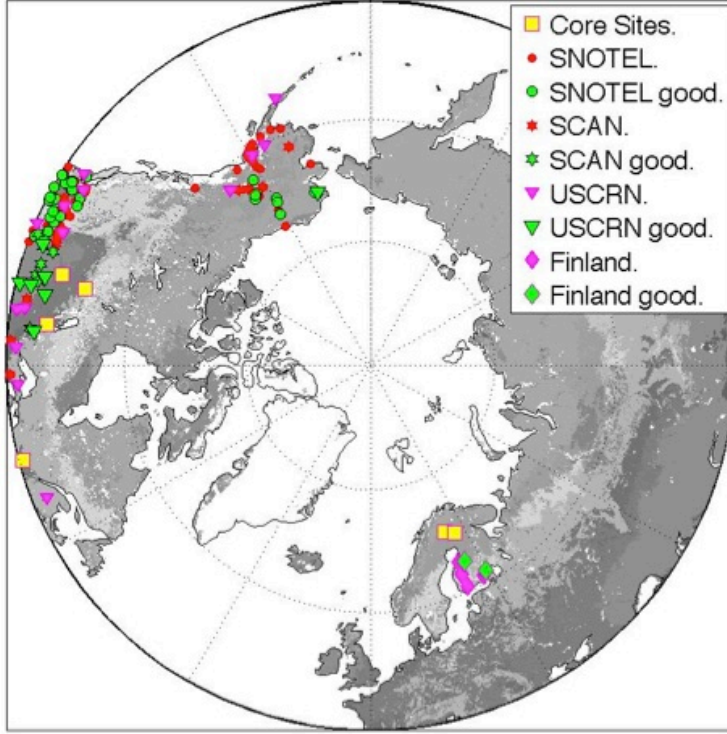


Figure 6. Freeze/thaw product cal/val sites (as of August 2014).

The computation of the classification accuracy proceeds as follows: Let $s_{AM/PM}(i,t) = 1$ if the L3_FT_A product at grid cell i (on the SMAP 3 km EASE grid) and time t indicates frozen conditions for AM (descending) or PM (ascending) overpass, respectively, and let $s_{AM/PM}(i,t) = 0$ if the L3_FT_A product indicates thawed conditions for AM or PM overpass, respectively. Likewise, let $v_{AM/PM}(i,t) = 1$ if the corresponding reference flag indicates frozen conditions at the AM or PM overpass, and $v(i,t) = 0$ for thawed conditions at the AM or PM overpass. Next, the error flag δ is set by comparing the SMAP product to the validating observations:

$$\delta_{AM/PM}(i,t) = \begin{cases} 0 & \text{if } s_{AM/PM}(i,t) = v_{AM/PM}(i,t) \\ 1 & \text{if } s_{AM/PM}(i,t) \neq v_{AM/PM}(i,t) \end{cases} \quad (7)$$

Note that a single L3_FT_A flag is produced each day, but is derived from separate descending (AM) and ascending (PM) overpasses. The L3_FT_A flags will therefore be separated back into binary freeze/thaw classes for the AM and PM orbits, producing two retrieval match-ups each day.

The mission Level 1 requirement will be satisfied if (for both AM and PM overpasses together):

$$1 - \left(\sum_{i=1}^{N_t} \sum_{t=1}^{N_t(i)} \delta(i,t) / \sum_{i=1}^{N_t} N_t(i) \right) \geq 0.8 \quad (8)$$

Equation 8 will be solved daily, to provide instantaneous determinations of freeze/thaw spatial accuracy, using the available reference sites. The mission requirement of 80% spatial accuracy will be assessed on a cumulative basis and for fixed monthly periods in order to provide overall product accuracy but reduce sensitivity to prolonged periods of consistent frozen and thawed states in the winter and summer, respectively. An example of pre-launch validation of an Aquarius derived freeze/thaw product using sparse observations from the NRCS SNOTEL network is shown in Table 6. The statistics were computed using data from 1 January to 15 June 2015, for 12 stations (8 in Alaska; 4 in the northwest U.S.). In this example, it is evident that the sole source of uncertainty in the Aquarius derived FT retrievals is the retrieval of thawed conditions when the reference data indicate frozen ground, likely due to the influence of wet snow on the radar signal. Uncertainty is highest during the period of seasonal transition from frozen to thawed conditions.

Table 6. Freeze/thaw flag agreement between Aquarius (AQ) and in situ (Obs) derived estimates. Agreement between the Aquarius derived FT and in situ FT flags computed relative to the total number of cases.

2014 SNOTEL vs. L3_FT_A_AQ	Agree All	Error All	AQ=F Obs=F	AQ=T Obs=T	AQ=F Obs=T	AQ=T Obs=F
January	0.96	0.04	0.96	0.00	0.00	0.04
February	1.00	0.00	1.00	0.00	0.00	0.00
March	0.94	0.06	0.86	0.08	0.00	0.06
April	0.73	0.27	0.59	0.14	0.00	0.27
May	0.62	0.38	0.07	0.55	0.00	0.38
June	0.92	0.08	0.00	0.92	0.00	0.08
Overall	0.87	0.13	0.63	0.24	0.00	0.13

Evaluation of the spatial classification accuracy with core validation sites and sparse networks is limited by the small number of reference pixels covered by these measurements (23 core reference pixels; 41 sparse network sites with optimal spatial representativeness as of August 2014). Daily comparison of the L3_FT_A freeze/thaw fields will therefore also be conducted with the modeled T_{surf} output (mean of skin temperature and 10 cm soil temperature) from the L3_SM_A product, but these results will not be used to formally assess the SMAP mission requirement for the freeze/thaw retrieval. As outlined in Figure 7, secondary data sources such as the GEOS-5 nature run will be used as supplemental information to expand the temporal and spatial domain of the validation, and for potential calibration of freeze/thaw dB reference states. The comparisons to supplemental information are expected to reveal potential inconsistencies in the product performance on the global scale not identifiable with point observations. In addition to the derivation of metrics with the in situ networks, two additional assessments will be performed.

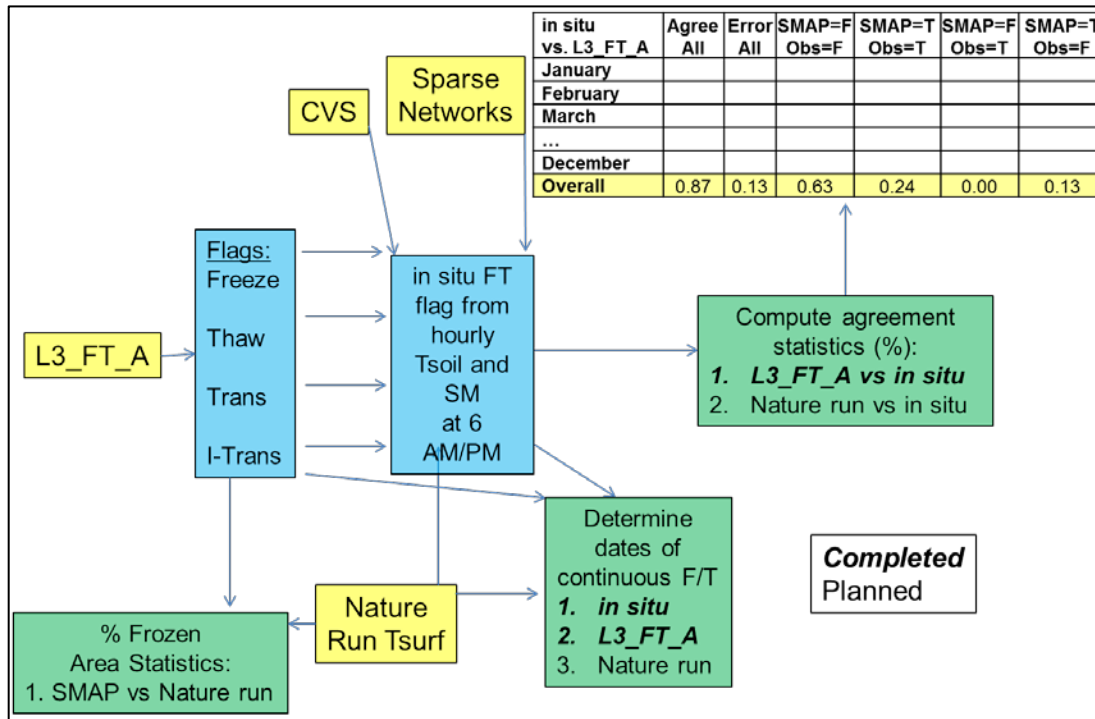


Figure 7. Overview of SMAP FT cal/val processes.

Below 45°N, the AM overpass radar freeze/thaw retrievals, implemented as a “frozen soil” flag in the L3_SM_A product, will be evaluated as part of the L4_C cal/val activities, primarily through pixel-point assessments with WMO daily air temperature measurements.

4.2.5 ALGORITHM BASELINE SELECTION

The current baseline algorithm is the algorithm of choice as it is best suited to fulfill mission requirements. Although aspects of the optional algorithms may be examined as part on on-going research, no changes are anticipated to the baseline algorithm prior to launch and operations.

5 CONSTRAINTS, LIMITATIONS, AND ASSUMPTIONS

Constraints and limitations of the algorithm will be assessed using the test procedures described above (e.g. Section 4.2.4). The landscape freeze/thaw state retrieval represented by the L3_FT_A algorithm and product characterizes the predominant frozen or non-frozen state of the land surface within the sensor field-of-view (FOV) and does not distinguish freeze/thaw characteristics among different landscape elements, including surface snow, soil, open water or vegetation. The lower frequency L-band SAR retrievals from SMAP are expected to have greater

sensitivity to surface soil freeze/thaw conditions under low to moderate vegetation cover, but effective radar penetration depth and microwave freeze/thaw sensitivity is strongly constrained by intervening vegetation biomass, soil moisture levels, and snow wetness. Ambiguity in relating changes in the radar signal to these specific landscape components is a challenge to validation of the FT product (Colliander et al., 2012). In northern, boreal and tundra landscapes L-band penetration depth and soil sensitivity is greater under frozen conditions when land surface liquid water levels are low, and markedly reduced under thawed conditions due to characteristically moist surface organic layer and soil active layer conditions, even under relatively low tundra vegetation biomass levels (Du et al. 2014).

The SMAP seasonal threshold freeze/thaw classification algorithm requires the establishment of accurate and stable frozen and non-frozen reference state dB conditions for each 3-km resolution grid cell. Initial reference conditions have been established pre-launch from relatively coarse (~100km) resolution Aquarius satellite L-band scatterometer measurements. The Aquarius data have a different sensor geometry and sampling, and a much coarser FOV than SMAP. The resulting freeze/thaw reference conditions determined from these data may cause significant SMAP freeze/thaw classification error, especially for areas with substantial sub-grid scale freeze/thaw heterogeneity relative to the coarse Aquarius FOV; sub-grid spatial heterogeneity will reduce dB differences between frozen and non-frozen reference states, leading to greater freeze/thaw classification uncertainty. The resulting spatial classification error is expected to be larger at lower latitudes (i.e. <math><45^{\circ}\text{N}</math>) where freeze/thaw is ephemeral and the difference between frozen and thawed radar references is relatively small, and over complex terrain where freeze/thaw heterogeneity is larger. The freeze/thaw accuracy of L3_FT_A and L3_SM_A products is expected to show substantial improvement during the SMAP post-launch period once a full seasonal cycle of successful SMAP observations is collected and used to define freeze/thaw reference conditions consistent with the SMAP L-band dB measurements.

The SMAP L-band SAR freeze/thaw retrievals will be determined using a 1-3km sensor FOV and mapped to a 3x3 km resolution product grid. The resulting freeze/thaw retrieval characterizes the predominant frozen or non-frozen condition of the landscape within a grid cell and does not distinguish sub-grid scale freeze/thaw heterogeneity within the sensor FOV. Previous studies using finer resolution (~100m) satellite L-band SAR (JERS-1 and PALSAR) data over Alaska indicate that freeze/thaw classification error from sub-grid scale heterogeneity is greater over complex terrain and during seasonal freeze/thaw transitions; spatial classification error decreases as the sensor footprint approaches the scale of landscape microclimate heterogeneity. The relative spatial classification error attributed to sub-grid scale heterogeneity under these conditions was determined to range up to approximately 15% for a 3-km sensor FOV and relative to a 100m baseline resolution (Du et al. 2014, Podest et al. 2014). The estimated contribution of sub-grid heterogeneity to the total freeze/thaw classification error was also found to be within the targeted 80% spatial accuracy threshold of the SMAP L3_FT_A product.

A major assumption of the seasonal threshold based temporal dB change freeze/thaw classification is that the major temporal shifts in radar backscatter are caused by land surface dielectric changes from temporal freeze/thaw transitions. This assumption generally holds for higher latitudes and elevations where seasonal frozen temperatures are a significant part of the annual cycle and a large constraint to land surface water mobility and ecosystem processes (e.g.,

Kim et al. 2012). However, freeze/thaw classification accuracy is expected to be reduced where other environmental factors may cause large temporal shifts in radar backscatter, including large rainfall events and surface inundation, and abrupt changes in vegetation biomass (e.g. phenology, disturbance and land cover change). Under relatively low land surface moisture levels, including arid and semi-arid zones, land surface dielectric changes and radar backscatter response to freeze/thaw transitions is reduced, and may be a secondary dielectric response compared to other environmental changes including seasonal precipitation variations; the freeze/thaw classification accuracy is expected to be reduced for these areas and conditions.

The SMAP L3_FT_A product distinguishes 4 levels of freeze/thaw conditions determined from the ascending (6AM) and descending (6PM) orbit SAR retrievals, including frozen (from both AM and PM overpass times), non-frozen (AM and PM), transitional (AM frozen; PM non-frozen) and inverse-transitional (AM non-frozen; PM frozen) states. The L3_FT_A product has sufficient fidelity and accuracy to distinguish diurnal freeze/thaw state changes common during seasonal transitions and temperate climate zones, and including frost-related impacts to vegetation productivity (e.g. Kim et al. 2014b). The SMAP L3_FT_A product will characterize diurnal freeze/thaw conditions over the northern ($\geq 45^\circ\text{N}$) domain, whereas the freeze/thaw retrievals and associated frozen flag in the L3_SM_A product will only be derived using the SMAP AM overpass data and will not be able to distinguish diurnal freeze/thaw state changes. The freeze/thaw classification results determined from the AM overpass SAR data are expected to show more frozen days over an annual cycle than the PM overpass retrievals for a given grid cell due to characteristic diurnal variations in solar radiation loading at the land surface and associated greater likelihood of maximum heating in the afternoon relative to morning.

6 REFERENCES

- Armstrong, R.L. and M. J. Brodzik. (1995) An Earth-gridded SSM/I data set for cryospheric studies and global change monitoring. *Advances in Space Research*, **16(10)**, 155-163.
- Betts, A. K., P. Viterbo, A. Beljaars, and B. van den Hurk. (2000) Impact of BOREAS on the ECMWF forecast model, *Journal of Geophysical Research*, **106(D24)**, 33,593-33,604.
- Black, T. A., W. Chen, A. Barr, A. Arain, Z. Chen, Z. Nesic, E. Hogg, H. Neumann, and P. Yang. (2000) Increased carbon sequestration by a boreal deciduous forest in years with a warm spring. *Geophysical Research Letters*, **27(9)**, 1271-1274.
- Churkina, G., and S. Running. (1998) Contrasting climatic controls on the estimated productivity of different biomes. *Ecosystems*, **1**, 206-215.
- Colliander, A., K. McDonald, R. Zimmermann, R. Schroeder, J. Kimball, and ENjoku. (2012) Application of QuikSCAT Backscatter to SMAP Validation Planning: Freeze/Thaw State Over ALECTRA Sites in Alaska From 2000 to 2007. *IEEE Transactions on Geoscience and Remote Sensing*, **50(2)**, 461-468.
- Du, J., J. S. Kimball, M. Azarderakhsh, R.S. Dunbar, M. Moghaddam, and K.C. McDonald. (2014) Classification of Alaska spring thaw characteristics using satellite L-band Radar remote sensing. *Transactions in Geoscience and Remote Sensing*, DOI:10.1109/TGRS.2014.2325409.

- Entekhabi, D., E. Njoku, P. Houser, M. Spencer, T. Doiron, J. Smith, R. Girard, S. Belair, W. Crow, T. Jackson, Y. Kerr, J. Kimball, R. Koster, K. McDonald, P. O'Neill, T. Pultz, S. Running, J.C. Shi, E. Wood, and J. Van Zyl. (2004) The Hydrosphere State (HYDROS) mission concept: An Earth System Pathfinder for global mapping of soil moisture and land freeze/thaw. *Transactions in Geoscience and Remote Sensing*, **42(10)**, 2184-2195.
- Entekhabi, D., E. Njoku, P. O'Neill, K. Kellogg, W. Crow, W. Edelstein, J. Entin, S. Goodman, T. Jackson, J. Johnson, J. Kimball, J. Piepmeier, R. Koster, K. McDonald, M. Moghaddam, S. Moran, R. Reichle, J. C. Shi, M. Spencer, S. Thurman, L. Tsang, J. Van Zyl. (2010) The Soil Moisture Active and Passive (SMAP) Mission. *Proceedings of the IEEE*, **98(5)**.
- Frolking S., K. McDonald, J. Kimball, R. Zimmermann, J.B. Way and S.W. Running. (1999). Using the space-borne NASA Scatterometer (NSCAT) to determine the frozen and thawed seasons of a boreal landscape. *Journal of Geophysical Research*, **104(D22)**, 27,895-27,907.
- Gamon, J.A., K.F. Huemmrich, J. Chen, D. Fuentes, F.G. Hall, J.S. Kimball, S. Goetz, J. Gu, K.C. McDonald, J.R. Miller, M. Moghaddam, D.R. Peddle, A.F. Rahman, J.-L. Roujean, E.A. Smith, C.L. Walthall, and P. Zarco-Tejada. (2004) Remote sensing in BOREAS: Lessons learned. *Remote Sensing of Environment*, **89(2)**, 139-162.
- Goulden, M.L., S. Wofsy, J. Harden, S. Trumbore, P. Crill, S. Gower, T. Fries, B. Daube, S. Fan, D. Sutton, A. Bazzaz, and J. Munger. (1998) Sensitivity of boreal forest carbon balance to soil thaw. *Science* **279(9)**, 214-217.
- Jarvis, P., and S. Linder. (2000) Constraints to growth of boreal forests. *Nature*, **405**, 904-905.
- Kim, Y., J.S. Kimball, K. Zhang, K. Didan, I. Velicogna, and K.C. McDonald. (2014a) Attribution of divergent northern vegetation growth responses to lengthening non-frozen seasons using satellite optical-NIR and microwave remote sensing. *International Journal of Remote Sensing*, **35(10)**, 3700-3721.
- Kim, Y., J. Kimball, K. Didan, and G. Henebry. (2014b) Response of vegetation growth and productivity to spring climate indicators in the conterminous United States derived from satellite remote sensing data fusion. *Agriculture And Forest Meteorology*, **194**, 132-143.
- Kim, Y., J.S. Kimball, K.C. McDonald and J. Glassy. (2011) Developing a global data record of daily landscape freeze/thaw status using satellite passive microwave remote sensing. *IEEE Transactions on Geoscience and Remote Sensing*, **49**, 949-960.
- Kim, Y., J. Kimball, K. Zhang, and K. McDonald. (2012) Satellite detection of increasing Northern Hemisphere non-frozen seasons from 1979 to 2008: Implications for regional vegetation growth. *Remote Sensing of Environment*, **121**, 472-487.
- Kimball, J., K. McDonald, A. Keyser, S. Frolking, and S. Running. (2001) Application of the NASA Scatterometer (NSCAT) for Classifying the Daily Frozen and Non-Frozen Landscape of Alaska, *Remote Sensing of Environment*, **75**, 113-126.
- Kimball, J.S., K.C. McDonald, S.W. Running, and S. Frolking. (2004a). Satellite radar remote sensing of seasonal growing seasons for boreal and subalpine evergreen forests. *Remote Sensing of Environment*, **90**, 243-258.
- Kimball, J.S., M. Zhao, K.C. McDonald, F.A. Heinsch, and S. Running. (2004b) Satellite observations of annual variability in terrestrial carbon cycles and seasonal growing seasons at high northern latitudes.

- In *Microwave Remote Sensing of the Atmosphere and Environment IV*, G. Skofronick Jackson and S. Uratsuka (Eds.), Proceedings of SPIE – The International Society for Optical Engineering, **5654**, 244-254.
- Kraszewski, A. (editor) (1996) *Microwave Aquametry: Electromagnetic Wave Interaction with Water-Containing Materials*, IEEE Press, Piscataway, N.J., 484 pp.
- Kuga, Y., M. Whitt, K. McDonald, F. and Ulaby. (1990) Scattering Models for Distributed Targets. In *Radar Polarimetry for Geoscience Applications*, Ulaby F. T. and Elachi C.,(Ed.), Artech House: Dedham, MA.
- McDonald, K.C. and J.S. Kimball. (2005) Hydrological application of remote sensing: Freeze-thaw states using both active and passive microwave sensors. In *Encyclopedia of Hydrological Sciences*. Vol. 5., M.G. Anderson and J.J. McDonnell (Eds.), John Wiley & Sons Ltd.
- McDonald, K.C., J.S. Kimball, E. Njoku, R. Zimmermann, and M. Zhao. (2004) Variability in springtime thaw in the terrestrial high latitudes: Monitoring a major control on the biospheric assimilation of atmospheric CO₂ with spaceborne microwave remote sensing. *Earth Interactions*, **8(20)**, 1-23.
- National Research Council. (2007) *Earth Science and Applications from Space: National Imperatives for the Next Decade and Beyond*. pp. 400.
- Nemani, R.R., C. Keeling, H. Hashimoto, W. Jolly, S. Piper, C. Tucker, R. Myneni, and S. Running. (2003) Climate-driven increases in global terrestrial net primary production from 1982 to 1999. *Science*, **300**, 1560-1563.
- Podest, E. (2006), *Monitoring Boreal Landscape Freeze/Thaw Transitions with Spaceborne Microwave Remote Sensing*. Ph.D. dissertation, University of Dundee.
- Podest, E., K.C. McDonald, and J.S. Kimball. (2014) Multi-sensor microwave sensitivity to freeze-thaw dynamics across a complex boreal landscape. *Transactions in Geoscience and Remote Sensing*, **52**, 6818-6828.
- Raney, K. R. (1998), Radar fundamentals: Technical perspective, In *Principles and Applications of Imaging Radar*, Vol. 2, F. M. Henderson and A. J. Lewis (Eds.), John Wiley and Sons Inc., New York, pp. 9-130.
- Rautiainen, K., J. Lemmetyinen, M. Schwank, A. Kontu, C. Ménard, C. Mätzler, M. Drusch, A. Wiesmann, J. Ikonen, and J. Pulliainen. (2014) Detection of soil freezing from L-band passive microwave observations, *Remote Sensing of Environment*, **147**, 206–218.
- Rawlins, M.A, K.C. McDonald, S. Frolking, R.B. Lammers, M. Fahnestock, J.S. Kimball, C.J. Vorosmarty. (2005) Remote Sensing of Pan-Arctic Snowpack Thaw Using the SeaWinds Scatterometer, *Journal of Hydrology*, **312/1-4**, 294-311.
- Rignot E., and Way, J.B. (1994) Monitoring freeze-thaw cycles along north-south Alaskan transects using ERS-1 SAR, *Remote Sensing of Environment*, **49**, 131-137.
- Rignot, E., Way, J.B., McDonald, K., Viereck, L., Williams, C., Adams, P., Payne, C., Wood, W., and Shi, J. (1994) Monitoring of environmental conditions in taiga forests using ERS-1 SAR, *Remote Sensing of Environment*, **49**, 145-154.
- Ulaby, F. T., R. Moore, and A. Fung. (1986) *Microwave Remote Sensing: Active and Passive, Vol. 1-3*, Artec House: Dedham MA.

Ulaby, F. T., K. Sarabandi, K. McDonald, M. Whitt, and M. Dobson. (1990). Michigan Microwave Canopy Scattering Model (MIMICS), *International Journal of Remote Sensing*, **11(7)**, 1223-1253.

Vaganov, E.A., M. Hughes, A. Kirilyanov, F. Schweingruber, and P. Silkin. (1999) Influence of snowfall and melt timing on tree growth in subarctic Eurasia. *Nature*, **400**, 149-151.

Way, J. B., J. Paris, E. Kasischke, C. Slaughter, L. Viereck, N. Christensen, M. Dobson, F. Ulaby, J. Richards, A. Milne, A. Sieber, F. Ahern, D. Simonett, R. Hoffer, M. Imhoff, and J. Weber. (1990) The effect of changing environmental conditions on microwave signatures of forest ecosystems: preliminary results of the March 1988 Alaskan aircraft SAR experiment. *International Journal of Remote Sensing*, **11**, 1119-1144.

Way, J. B., R. Zimmermann, E. Rignot, K. McDonald, and R. Oren. (1997) Winter and Spring Thaw as Observed with Imaging Radar at BOREAS, *Journal of Geophysical Research*, **102(D24)**, 29673-29684.

Wegmuller, U. (1990), The effect of freezing and thawing on the microwave signatures of bare soil, *Remote Sensing of Environment*, **33**, 123-135.

Wismann, V. (2000) Monitoring of seasonal thawing in Siberia with ERS scatterometer data. *IEEE Transactions on Geoscience and Remote Sensing*, **38**, 1804–1809.

APPENDIX 1: GLOSSARY

[Adapted from: Earth Observing System Data and Information System (EOSDIS) Glossary <http://www-v0ims.gsfc.nasa.gov/v0ims/DOCUMENTATION/GLOS-ACR/glossary.of.terms.html>.]

ALGORITHM. (1) Software delivered by a science investigator to be used as the primary tool in the generation of science products. The term includes executable code, source code, job control scripts, as well as documentation. (2) A prescription for the calculation of a quantity; used to derive geophysical properties from observations and to facilitate calculation of state variables in models.

ANCILLARY DATA. Data other than instrument data required to perform an instrument's data processing. They include orbit data, attitude data, time information, spacecraft engineering data, calibration data, data quality information, data from other instruments (spaceborne, airborne, ground-based) and models.

BROWSE. A representation of a data set or data granule used to pre-screen data as an aid to selection prior to ordering. A data set, typically of limited size and resolution, created to rapidly provide an understanding of the type and quality of available full resolution data sets. It may also enable the selection of intervals for further processing or analysis of physical events. For example, a browse image might be a reduced resolution version of a single channel from a multi-channel instrument. Note: Full resolution data sets may be browsed.

BROWSE DATA PRODUCT. Subsets of a larger data set, generated for the purpose of allowing rapid interrogation (i.e., browse) of the larger data set by a potential user. For example, the browse product for an image data set with multiple spectral bands and moderate spatial resolution might be an image in two spectral channels, at a degraded spatial resolution. The form of browse data is generally unique for each type of data set and depends on the nature of the data and the criteria used for data selection within the relevant scientific disciplines.

Dynamic Browse. Refers to the generation of a browse product, including subsetting and/or resampling of data, by command of the user engaged in the browse activity. The browse data set is built in real-time, or near-real-time, as part of the browse activity.

Static Browse. Refers to interrogation of browse products which have been generated (through subsetting and/or resampling) before any user browses that particular data set.

CALIBRATION. (1) The activities involved in adjusting an instrument to be intrinsically accurate, either before or after launch (i.e., "instrument calibration"). (2) The process of collecting instrument characterization information (scale, offset, nonlinearity, operational, and environmental effects), using either laboratory standards, field standards, or modeling, which is used to interpret instrument measurements (i.e., "data calibration").

CALIBRATION DATA. The collection of data required to perform calibration of the instrument science and engineering data, and the spacecraft or platform engineering data. It includes pre-flight calibrator measurements, calibration equation coefficients derived from calibration software routines, and ground truth data that are to be used in the data calibration processing routine.

CORRELATIVE DATA. Scientific data from other sources used in the interpretation or validation of instrument data products, e.g. ground truth data and/or data products of other instruments. These data are not utilized for processing instrument data.

DATA PRODUCT. A collection (1 or more) of parameters packaged with associated ancillary and labeling data. Uniformly processed and formatted. Typically uniform temporal and spatial resolution. (Often the collection of data distributed by a data center or subsetted by a data center for distribution.) There are two types of data products:

Standard - A data product produced by a community consensus algorithm. Typically produced for a wide community. May be produced routinely or on-demand. If produced routinely, typically produced over most or all of the available independent variable space. If produced on-demand, produced only on request from users for particular research needs typically over a limited range of independent variable space.

Special - A data product produced by a research status algorithm. May migrate to a community consensus algorithm at a later time. If adequate community interest exists, the product may be archived and distributed by a DAAC.

DATA PRODUCT LEVEL. Data levels 1 through 4 as designated in the EOSDIS Product Type and Processing Level Definitions document.

Raw Data - Data in their original packets, as received from the observer, unprocessed.

Level 0 - Raw instrument data at original resolution, time ordered, with duplicate packets removed.

Level 1A - Reconstructed unprocessed instrument data at full resolution, time referenced, and annotated with ancillary information, including radiometric and geometric calibration coefficients and georeferencing parameters (i.e., platform ephemeris) computed and appended, but not applied to Level 0 data.

Level 1B - Radiometrically corrected and geolocated Level 1A data that have been processed to sensor units.

Level 1C - Level 1B data that have been spatially resampled.

Level 2 - Derived geophysical parameters at the same resolution and location as the Level 1 (1B or 1C) data.

Level 3 - Geophysical or sensor parameters that have been spatially and/or temporally re-sampled (i.e., derived from Level 2 or Level 1 data).

Level 4 - Model output and/or results of lower level data that are not directly derived by the instruments.

DISTRIBUTED ACTIVE ARCHIVE CENTER (DAAC). An EOSDIS facility that archives, and distributes data products, and related information. An EOSDIS DAAC is managed by an institution such as a NASA field center or a university, under terms of an agreement with NASA. Each DAAC contains functional elements for archiving and disseminating data, and for user services and information management. Other (non-NASA) agencies may share management and funding responsibilities for the active archives under terms of agreements negotiated with NASA.

GRANULE. The smallest aggregation of data which is independently managed (i.e., described, inventoried, retrievable). Granules may be managed as logical granules and/or physical granules.

GUIDE. A detailed description of a number of data sets and related entities, containing information suitable for making a determination of the nature of each data set and its potential usefulness for a specific application.

INSTRUMENT DATA. Data specifically associated with the instrument, either because they were generated by the instrument or included in data packets identified with that instrument. These data consist of instrument science and engineering data, and possible ancillary data.

Instrument Engineering Data. Data produced by the engineering sensor(s) of an instrument that is used to determine the physical state of an instrument in order to operate it, monitor its health, or aid in processing its science data.

Instrument Science Data. Data produced by the science sensor(s) containing the primary observables of an instrument, usually constituting the mission of that instrument.

METADATA. (1) Information about a data set which is provided by the data supplier or the generating algorithm and which provides a description of the content, format, and utility of the data set. Metadata provide criteria which may be used to select data for a particular scientific investigation. (2) Information describing a data set, including data user guide, descriptions of the data set in directories, and inventories, and any additional information required to define the relationships among these.

NEAR REAL-TIME DATA. Data from the source that are available for use within a time that is short in comparison to important time scales in the phenomena being studied.

ORBIT DATA. Data that represent spacecraft locations. Orbit (or ephemeris) data include: Geodetic latitude, longitude and height above an adopted reference ellipsoid (or distance from the center of mass of the Earth); a corresponding statement about the accuracy of the position and the corresponding time of the position (including the time system); some accuracy requirements may be hundreds of meters while other may be a few centimeters.

PARAMETER. A measurable or derived variable represented by the data (e.g. air temperature, snow depth, relative humidity).

QUICK-LOOK DATA. Data available for examination within a short time of receipt, where completeness of processing is sacrificed to achieve rapid availability.

RAW DATA. Numerical values representing the direct observations output by a measuring instrument transmitted as a bit stream in the order they were obtained. (Also see DATA PRODUCT LEVEL.)

REAL-TIME DATA. Data that are acquired and transmitted immediately to the ground (as opposed to playback data). Delay is limited to the actual time (propagation delays) required to transmit the data.

SPACECRAFT ENGINEERING DATA. Data produced by the engineering sensor(s) of a spacecraft that are used to determine the physical state of the spacecraft, in order to operate it or monitor its health.